Appendix A.44:

Hillmorton High School – VsVp 57201

Table 1: Site Description for Hillmorton High School (VsVp 57201).

Attribute	Yes/No			Description/Date	Symbol in Figure 1
	10-m Buffer	20-m Buffer	50-m Buffer		
Near a body of surface water or other free face features?	No	No	No	The center of the site is ~260 m to the SW (the free-face height is ~1 m) and ~385 m (the free-face height is ~2.5 m) to the SE from the Heathcote River.	NA
Lateral spreading observed during the CES?	No	No	No	Lateral spreading was not observed by the mapping team.[1]	NA
Nearby buildings or structures?	No	Yes	Yes	Building coverage of the 20- and 50-m buffers is 14 and 21%, respectively. The buildings are in the SE and SW quadrants of the 20-m buffer and all quadrants of the 50-m buffer.	White Fill + Brown Outline
Sloping land?	No	No	No	Flat land, open field + residential area	NA
Step changes in the ground surface?	No	No	No	NA	NA
Retaining walls?	No	No	No	NA	NA
Vegetation?	Yes	Yes	Yes	Trees and bushes cover 18, 39, and 32% of the 10-, 20-, and 50-m buffers, respectively. They are in the NE, NW, and SW quadrants of the 10- and 20-m buffers and all quadrants of the 50-m buffer.	White Fill + Green Outline
Anthropogenic changes to the site between the LiDAR surveys?	Yes	Yes	Yes	Vegetation removal in the S portion of the 50-m buffer between Jan 2007 and Mar 2009. Vegetation replacement and earthwork in the N portion of all buffers. Vegetation removal in the SE portion of the 50-m buffer between Oct 2012 and Jan 2013. Building removal in the S portion of the 20- and 50-m buffers between Aug 2013 and Jan 2014.	Earthwork: Orange Outline + White Fill; Building Removal: Orange Crossline; Vegetation Removal: Green Crossline
Other important factors?	Yes	Yes	Yes	There is a possibility the field was re-grassed between July 2003 and Nov 2015, which would affect all quadrants of all buffers and LiDAR measurements. Above-ground water pipes or similar in the NE quadrant of the 50-m buffer. Uneven surface in the NW quadrant of all buffers.	NA

Note: Buffer is the area within a circle of a specified radius with CPT investigations done at its center (172.593252°, -43.556187°).

[1] Canterbury Geotechnical Database. (2012). "Observed Ground Crack Locations", Map Layer CGD0400 - 23 July 2012, retrieved July 09, 2018 from https://canterburygeotechnicaldatabase.projectorbit.com/

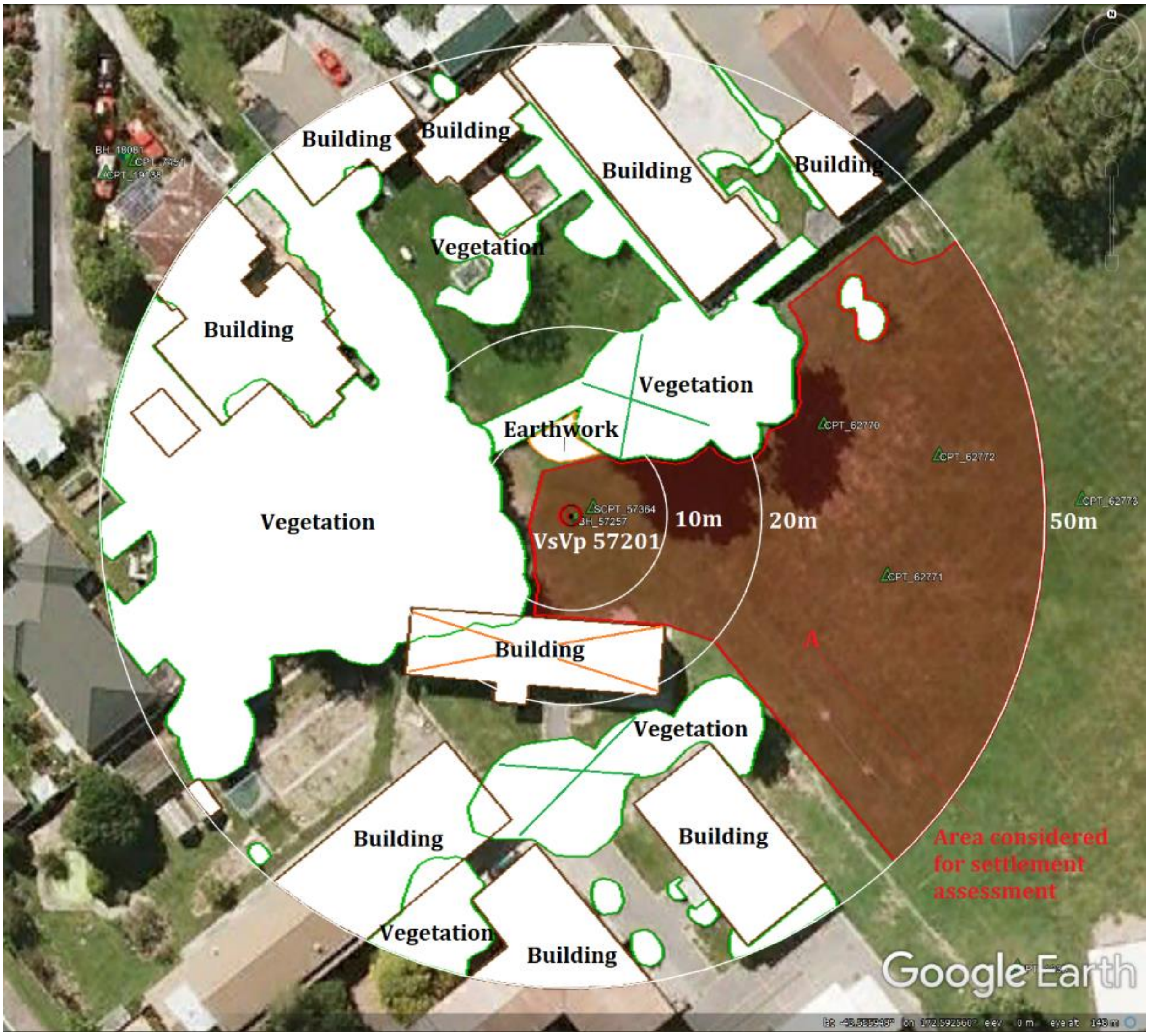

Figure 1: Site plan with areas where ejecta-induced settlement is considered.

Note 1: Patch A (outlined in red) in free field was selected for settlement assessment as an area free of vegetation and structures. Other important factors considered for the patch selection were its proximity to a CPT, a property subjected to addition and/or demolition of a structure, front yard/backyard alterations (e.g., ploughing, rubble, scrap), and aerial distribution of sediment ejecta. The LiDAR-based settlement analyses were not conducted for any earthquake event due to the evident absence of ejecta from Patch A for the Sep-10, Jun-11, and Dec-11 EQs and the unavailability of the Sep-10 LiDAR survey used to compute the ground surface subsidence for the Feb-11 EQ.

Table 2: LiDAR flight error adjustments, global adjustments for the difference between average LiDAR point elevations and benchmark survey elevations, and vertical tectonic movement adjustments.

	Adjustments (mm)		
Earthquake Event(s)	LiDAR Flight Error	Global Offset[2]	Tectonic Vertical Movement
Sep-10	NA	-3	0
Feb-11	NA	16	-50
Jun-11	0	38	-15
Dec-11	NA	-65	0
CES	NA	-14	-65
Any LiDAR survey affected by ejecta?			No

Note: The negative sign indicates the subtraction from the ground surface subsidence, while the positive sign indicates the addition to the ground surface subsidence.

Table 3: LiDAR Measurement Error for Patch A.

Surveys	Buffer	Area Averaged Difference Indicating Repeat Measurement Error (mm)	$\sigma^*_{\text{individual LiDAR points}}$ (mm)	%Reduction in σ due to Area Averaging of LiDAR Points
Post Feb 2011: Mar 2011 and May 2011	10-m	ND	59	[ND,ND]
	20-m	ND		
	50-m	ND		
Post Dec 2011: Feb 2012 and Oct 2015	10-m	NA	70	[NA,NA]
	20-m	NA		
	50-m	NA		

*Standard deviation.

[2] Russell, J., & van Ballegooy, S. (2015). *Canterbury Earthquake Sequence: Increased liquefaction vulnerability assessment methodology*. New Zealand: Tonkin & Taylor Ltd.

Table 4: Ground surface subsidence adjustments due to LiDAR measurement error for Patch A.

Earthquake Event(s)	$\sigma_{\text{pre-EQ LiDAR survey}}$ (mm)	$\sigma_{\text{post-EQ LiDAR survey}}$ (mm)	σ_{total} (mm)	Area Average Adjusted σ (mm) **
Sep-10	158	56	134	ND
Feb-11	56	59	59	ND
Jun-11	59	61	62	ND
Dec-11	61	70	87	ND
CES	158	70	124	ND

**Based on the highest %Reduction in Table 3.

Table 5: Raw liquefaction-related ground surface subsidence using original LiDAR points for Patch A.

	Average Ground Surface Subsidence (mm)		
Earthquake Event(s)	10-m Buffer	20-m Buffer	50-m Buffer
Sep-10	NA	NA	NA
Feb-11	NA	NA	NA
Jun-11	ND	ND	ND
Dec-11	NA	NA	NA
CES	NA	NA	NA

Table 6: Corrected liquefaction-related ground surface subsidence using original LiDAR points for Patch A with the calculated adjustments in Table 2.

	Average Calculated Ground Surface Subsidence (mm)		
Earthquake Event(s)	10-m Buffer	20-m Buffer	50-m Buffer
Sep-10	NA	NA	NA
Feb-11	NA	NA	NA
Jun-11	ND	ND	ND
Dec-11	NA	NA	NA
CES	NA	NA	NA

Notes: Plus/minus values are same as those in Table 4, but rounded to the nearest 25 mm; Positive overall values indicate ground surface subsidence, while negative overall values indicate ground surface uplift; NA = Not available; ND = Not determined.

Table 7: Corrected liquefaction-related ground surface subsidence for Patch A using LiDAR DEMs.

	Estimated Ground Surface Subsidence (mm)								
	10-m Buffer			20-m Buffer			50-m Buffer		
Earthquake Event(s)	16th %ile	50th %ile	84th %ile	16th %ile	50th %ile	84th %ile	16th %ile	50th %ile	84th %ile
Sep-10	NA	NA	NA	NA	NA	NA	NA	NA	NA
Feb-11	NA	NA	NA	NA	NA	NA	NA	NA	NA
Jun-11	<50	<50	<50	<50	<50	<50	<50	<50	<50
Dec-11	NA	NA	NA	NA	NA	NA	NA	NA	NA
CES	NA	NA	NA	NA	NA	NA	NA	NA	NA

Note: These percentiles are not the exact statistical measures; they indicate the spatial variability of ground surface subsidence.

Table 8a: Ejecta-Induced settlement for the top 20 m of the soil profile for Patch A (10-m buffer) for the 50th %ile PGA, P_L=50%, and C_{FC}=0.13 using BI-2014, ZRB-2002, and I_C cutoff of 2.6.

Earthquake Event(s)	M_W	PGA (g)	Depth to Groundwater (m)	S_T (mm)	S_{V1D} (mm)	$S_{E,L}$ (mm)
Sep-10	7.1	0.24	2.7	NA	161±20	NA
Feb-11	6.2	0.40	2.7	NA	192±50	NA
Jun-11	6.2	0.18	2.5	ND	42±25	ND
Dec-11	6.1	0.14	2.7	NA	4±50	NA

Notes: S_T = Total settlement (Table 6); S_{V1D} = Average vertical settlement due to volumetric compression using Boulanger and Idriss (2014) (BI-2014), Zhang et al. (2002) (ZRB-2002) procedures and de Greef and Lengkeek (2018) thin-layer correction; $S_{E,L}$ = Ejecta-induced settlement as the difference between the LiDAR-based S_T and S_{V1D}.

Table 8b: Ejecta-Induced settlement for the top 20 m of the soil profile for Patch A (20-m buffer) for the 50th %ile PGA, P_L=50%, and C_{FC}=0.13 using BI-2014, ZRB-2002, and I_C cutoff of 2.6.

Earthquake Event(s)	M_W	PGA (g)	Depth to Groundwater (m)	S_T (mm)	S_{V1D} (mm)	$S_{E,L}$ (mm)
Sep-10	7.1	0.24	2.7	NA	170±20	NA
Feb-11	6.2	0.40	2.7	NA	206±50	NA
Jun-11	6.2	0.18	2.5	ND	42±25	ND
Dec-11	6.1	0.14	2.7	NA	4±50	NA

Notes: S_T = Total settlement (Table 6); S_{V1D} = Average vertical settlement due to volumetric compression using Boulanger and Idriss (2014) (BI-2014), Zhang et al. (2002) (ZRB-2002) procedures and de Greef and Lengkeek (2018) thin-layer correction; $S_{E,L}$ = Ejecta-induced settlement as the difference between the LiDAR-based S_T and S_{V1D}.

Table 8c: Ejecta-Induced settlement for the top 20 m of the soil profile for Patch A (50-m buffer) for the 50th %ile PGA, P_L=50%, and C_{FC}=0.13 using BI-2014, ZRB-2002, and I_C cutoff of 2.6.

Earthquake Event(s)	M_W	PGA (g)	Depth to Groundwater (m)	S_T (mm)	S_{V1D} (mm)	$S_{E,L}$ (mm)
Sep-10	7.1	0.24	2.7	NA	159±20	NA
Feb-11	6.2	0.40	2.7	NA	197±50	NA
Jun-11	6.2	0.18	2.5	ND	39±25	ND
Dec-11	6.1	0.14	2.7	NA	3±50	NA

Notes: S_T = Total settlement (Table 6); S_{V1D} = Average vertical settlement due to volumetric compression using Boulanger and Idriss (2014) (BI-2014), Zhang et al. (2002) (ZRB-2002) procedures and de Greef and Lengkeek (2018) thin-layer correction; $S_{E,L}$ = Ejecta-induced settlement as the difference between the LiDAR-based S_T and S_{V1D}.

Note 2: The uncertainty for volumetric settlement was derived based on the sensitivity of volumetric settlement to PGA, C_{FC}, and P_L for each earthquake event for VsVp 57203 *Shirley Intermediate School* and CC LIQ 1 – CPT 5586 – *Vivian St* sites. Taking the 50th percentile as the baseline case, the minimum and maximum values corresponding to the difference between the 25th percentile and the 50th percentile and the 75th percentile and the 50th percentile were determined. The arithmetic mean of the range of the minimum and maximum difference was evaluated for each patch at the two sites. The maximum arithmetic mean for each earthquake event was rounded to the nearest five and used as the uncertainty value. Accordingly, the 1-D volumetric settlement uncertainties of ±20, ±50, ±25, and ±50 mm for the Sep-10, Feb-11, Jun-11, and Dec-11 earthquake events, respectively, were used for all sites in this study.

Table 9a: Coverage area and height of ejecta estimates for Patch A (10-m buffer) using photographs.

Earthquake Event	$A_{E,thick}$ (m^2)	$H_{E,thick}$ (mm)	$V_{E,cone}$ (m^3)	$H_{E,cone}$ (mm)	A_T (m^2)
Sep-10	0	0	0	0	191
Feb-11	6.3	100-200	0.8-1.1	200-300	191
Jun-11	0	0	0	0	191
Dec-11	0	0	0	0	191

Notes: $A_{E,thick/thin}$ = Coverage area of thick/thin ejecta layers; $H_{E,thick/thin}$ = Lower-upper estimate of height of thick/thin ejecta layers; $A_{E,cone}$ = Coverage area of conically shaped ejecta layers; $H_{E,cone}$ = Lower-upper estimate of height of conically shaped ejecta layers; A_T = Total assessment area of a buffer being considered; Thin and thick layers correspond to light gray and dark gray colors of ejecta observed in aerial photographs.

Table 9b: Coverage area and height of ejecta estimates for Patch A (20-m buffer) using photographs.

Earthquake Event	$H_{E,cone}$ (mm)	$V_{E,cone}$ (m²)	$H_{E,thick}$ (mm)	$A_{E,thick}$ (m²)	$H_{E,thin}$ (mm)	$A_{E,thin}$ (m²)	A_T (m²)
Sep-10	0	0	0	0	0	0	398
Feb-11	200-300	2.8-4.1	100-200	6.3	10-30	13.2	379*
Jun-11	0	0	0	0	0	0	398
Dec-11	0	0	0	0	0	0	398

Notes: $A_{E,thick/thin}$ = Coverage area of thick/thin ejecta layers; $H_{E,thick/thin}$ = Lower-upper estimate of height of thick/thin ejecta layers; Thin and thick layers correspond to light gray and dark gray colors of ejecta observed in aerial photographs; $H_{E,cone}$ = Lower-upper estimate of height of conically shaped ejecta layers; $A_{E,cone}$ = Coverage area of conically shaped ejecta layers; A_T = Total assessment area of a buffer being considered; * indicates the reduction in A_T due to the presence of shadows.

Table 9c: Coverage area and height of ejecta estimates for Patch A (50-m buffer) using photographs.

EQ Event	$H_{E,thin}$ (mm)	$A_{E,thin}$ (m²)	$H_{E,thick}$ (mm)	$A_{E,thick}$ (m²)	H_{E,c_thin} (mm)	V_{E,c_thin} (m³)	H_{E,c_thick} (mm)	V_{E,c_thick} (m³)	A_T (m²)
Sep-10	0	0	0	0	0	0	0	0	1893
Feb-11	10-30	110.2	100-200	23.9	80-160	0.1-0.2	200-300	6.8-10.1	1875*
Jun-11	0	0	0	0	0	0	0	0	1893
Dec-11	0	0	0	0	0	0	0	0	1893

Notes: $H_{E,c\_thick/thin}$ = Lower-upper estimate of height of thick/thin conically shaped ejecta layers; $A_{E,c\_thick/thin}$ = Coverage area of thick/thin conically shaped ejecta layers; $A_{E,thick/thin}$ = Coverage area of thick/thin ejecta layers; $H_{E,thick/thin}$ = Lower-upper estimate of height of thick/thin ejecta layers; Thin and thick layers correspond to light gray and dark gray colors of ejecta observed in aerial photographs; A_T= Total assessment area of a buffer being considered; * indicates the reduction in A_T due to the presence of shadows.

Note 3: The values in Table 9 correspond to the coverage area of ejecta outlined in aerial photographs (Figures 22, 23, 25, and 37) and the lower and upper estimates of ejecta height based on ground photographs (Figure 38) and EQC LDAT property inspection reports. The ejecta-induced settlement using photographs and engineering judgment, $S_{E,P}$, is estimated as

$$S_{E,P} = \frac{\sum_{i=1}^{a} A_{E,thick,i} * H_{E,thick,i} + \sum_{j=1}^{b} A_{E,thin,j} * H_{E,thin,j}}{A_T} + \frac{\frac{1}{3}\sum_{m=1}^{e} A_{E,c\_thick,m} * H_{E,c\_thick,m} + \frac{1}{3}\sum_{n=1}^{f} A_{E,c\_thin,n} * H_{E,c\_thin,n}}{A_T} = \frac{\sum_{i=1}^{a} V_{E,thick,i} + \sum_{j=1}^{b} V_{E,thin,j} + \sum_{m=1}^{e} V_{E,c\_thick,m} + \sum_{n=1}^{f} V_{E,c\_thin,n}}{A_T}$$

where

- $A_{E,thick,i}$ and $H_{E,thick,i}$ are the area and the height of a thick ejecta layer, respectively;
- $A_{E,thin,j}$ and $H_{E,thin,j}$ are the area and the height of a thin ejecta layer, respectively;

- $A_{E,c\_thick,m}$ and $H_{E,c\_thick,m}$ are the aerea and the height of a thick conically shaped ejecta, respectively;
- $A_{E,c\_thin,n}$ and $H_{E,c\_thin,n}$ are the area and the height of a thin conically shaped ejecta, respectively;
- A_T is the total assessment area for a buffer being considered (Figure 1).

Table 10: Ejecta-induced settlement estimates for Patch A based on photographs.

Earthquake Event	Patch A (10-m buffer)		Patch A (20-m buffer)		Patch A (50-m buffer)	
	$S_{E,P,lower}$ (mm)	$S_{E,P,upper}$ (mm)	$S_{E,P,lower}$ (mm)	$S_{E,P,upper}$ (mm)	$S_{E,P,lower}$ (mm)	$S_{E,P,upper}$ (mm)
Sep-10	0	0	0	0	0	0
Feb-11	7	13	9	15	6	10
Jun-11	0	0	0	0	0	0
Dec-11	0	0	0	0	0	0

Note: $S_{E,P,lower}$ and $S_{E,P,upper}$ correspond to lower and upper estimates of $S_{E,P}$, respectively.

Table 11: Best final estimates of ejecta-induced settlement for Patches A, B, and C.

EQ Event	Patch A (10-m buffer)			Patch A (20-m buffer)			Patch A (50-m buffer)		
	$S_{E,L}$ (mm)	$S_{E,P}$ (mm)	$S_{E,final}$ (mm)	$S_{E,L}$ (mm)	$S_{E,P}$ (mm)	$S_{E,final}$ (mm)	$S_{E,L}$ (mm)	$S_{E,P}$ (mm)	$S_{E,final}$ (mm)
Sep-10	NA	0	0	NA	0	0	NA	0	0
Feb-11	NA	10 ± 3	10 ± 5	NA	12 ± 3	10 ± 5	NA	8 ± 2	10 ± 5
Jun-11	ND	0	0	ND	0	0	ND	0	0
Dec-11	NA	0	0	NA	0	0	NA	0	0

Notes: $S_{E,L}$ = Ejecta-induced settlement based on LiDAR data reported in Table 8; $S_{E,P}$ = Median ejecta-induced settlement for the range of values reported in Table 10; $S_{E,final}$ = Best final estimate of ejecta-induced settlement rounded to the nearest 5 mm; Final plus/minus values are also rounded to the nearest 5 mm; NA = Not available; ND = Not determined.

Note 4:

- $S_{E,final}$ for Patch A is based solely on $S_{E,P}$ for all earthquake events due to the evident absence of ejecta for the Sep-10, Jun-11, and Dec-11 EQs and unavailability of $S_{E,L}$ for the Feb-11 EQ. The uncertainty associated with $S_{E,final}$ for Patch A is also based on the uncertainty associated with $S_{E,P}$ for all earthquake events.
- The site in in the zone of excessive LPI overprediction of liquefaction severity for the Sep-10 and Feb-11 EQ (Maurer et al. 2014[3]).
- The LDAT property inspection reports are available for nearby properties where the maximum ejecta height was reported as 300 mm in Oct 2011. There are no ground photographs of the site.

[3] Maurer, B. W., Green, R. A., Cubrinovski, M., & Bradley, B. A. (2014). Evaluation of the Liquefaction Potential Index for Assessing Liquefaction Hazard in Christchurch, New Zealand. *Journal of Geotechnical and Geoenvironmental Engineering*, 140(7), 04014032-1-11. doi:10.1061/(asce)gt.1943-5606.0001117

<u>Summary 1</u>:

The best estimate of the ejecta-induced free-field ground settlement at the Hillmorton High School site for the SEP 2010, FEB, JUN 2011, and DEC 2011 earthquake is 0 mm, 10±5 mm, 0 mm, and 0 mm, respectively.

Figure 2: Location of the site.

Figure 3: Position of the site relative to nearby buildings, vegetation, and free-face features.

Figure 4: Street view of the nearby flat land.

Figure 5: Satellite image of the site taken in Apr 2004.

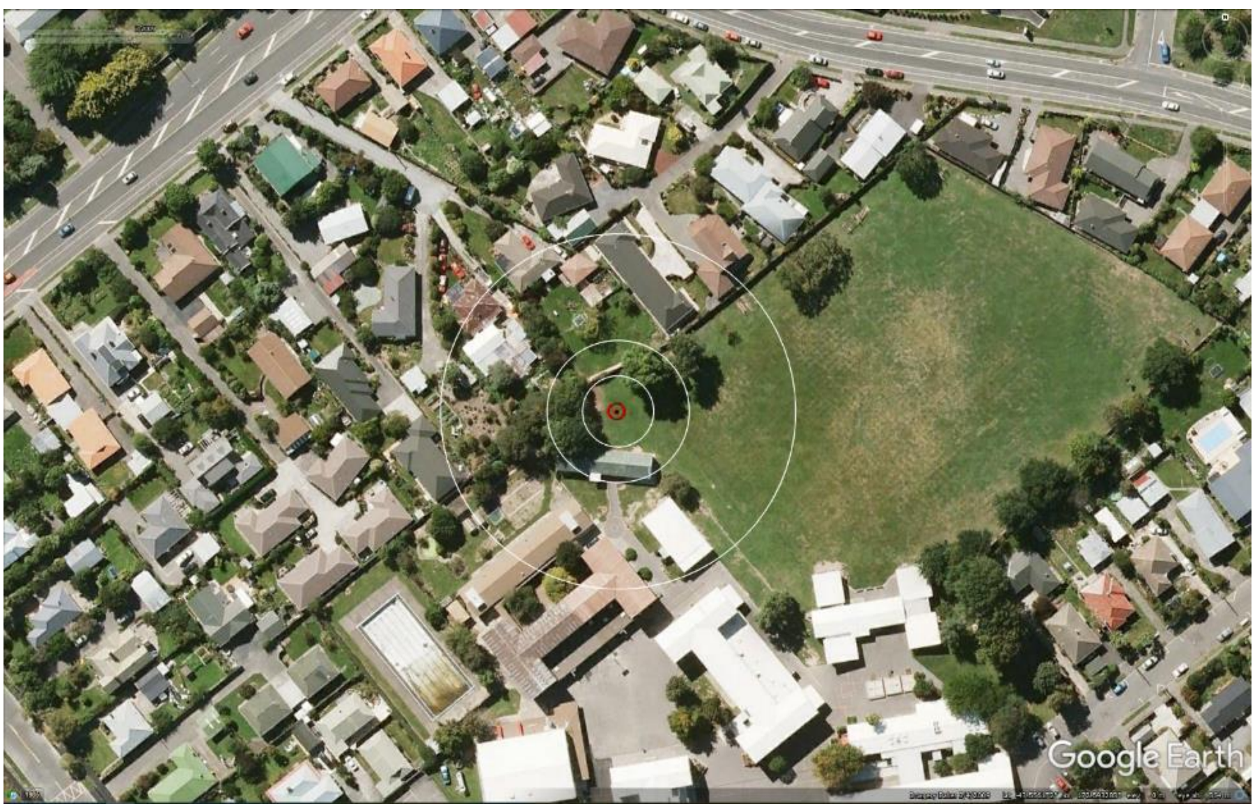

Figure 6: Satellite image of the site taken in Mar 2009.

Figure 7: Satellite image of the site taken on Sep 3, 2010.

Figure 8: Satellite image of the site taken on Sep 5, 2010.

Figure 9: Satellite image of the site taken on Feb 15, 2011.

Figure 10: Satellite image of the site taken on Feb 23, 2011.

Figure 11: Satellite image of the site taken on Feb 26, 2011.

Figure 12: Satellite image of the site taken on Mar 28, 2011.

Figure 13: Satellite image of the site taken on Aug 30, 2011.

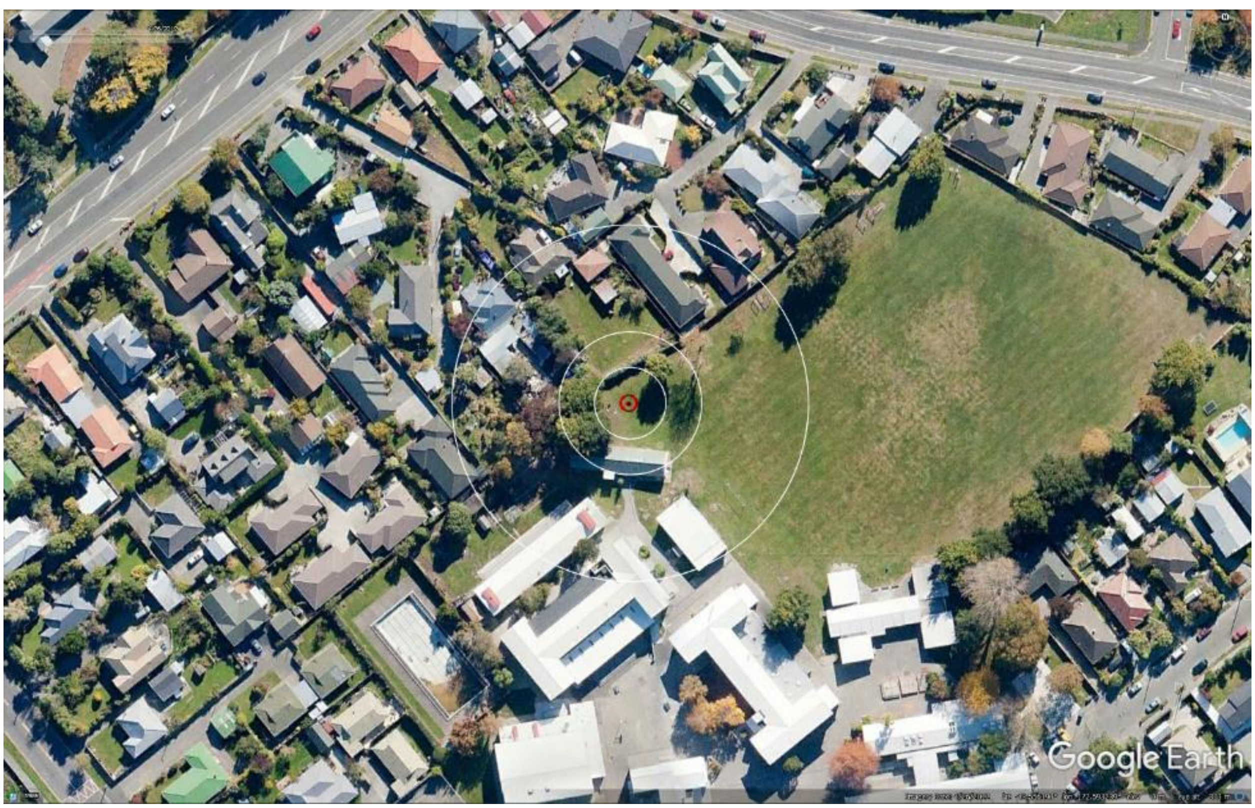

Figure 14: Satellite image of the site taken in Apr 2012.

Figure 15: Satellite image of the site taken in Oct 2012.

Figure 16: Satellite image of the site taken in Jan 2013.

Figure 17: Satellite image of the site taken in Aug 2013.

Figure 18: Satellite image of the site taken in Jan 2014.

Figure 19: Satellite image of the site taken in Nov 2015.

Figure 20: Aerial photograph of the site taken on Sep 4, 2010.

Figure 21: Aerial photograph of the site taken on Feb 24, 2011.

Figure 22: Aerial photograph of the site taken on June 14-15, 2011 (zoomed out).

Figure 23: Aerial photograph of the site taken on June 14-15, 2011 (zoomed in).

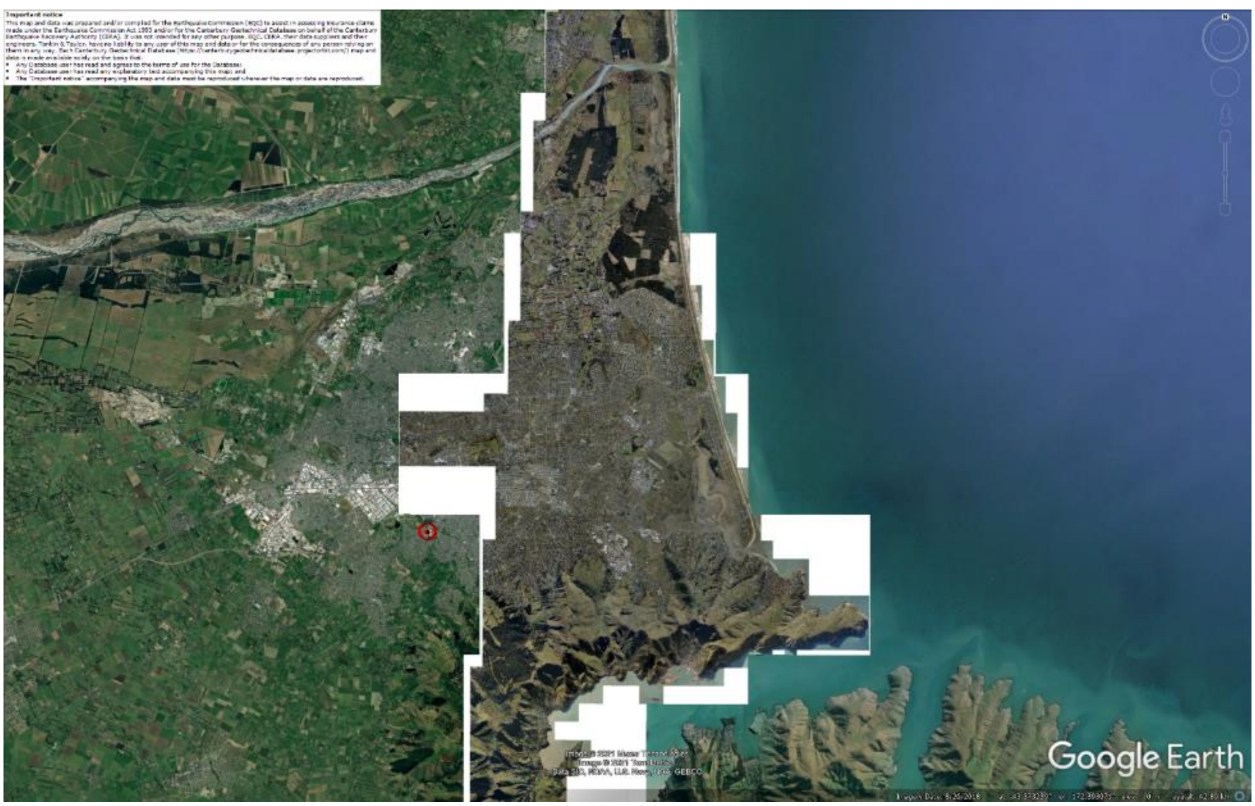

Figure 24: Aerial photograph of the site taken on June 16, 2011.

Figure 25: Aerial photograph of the site taken on Dec 24, 2011.

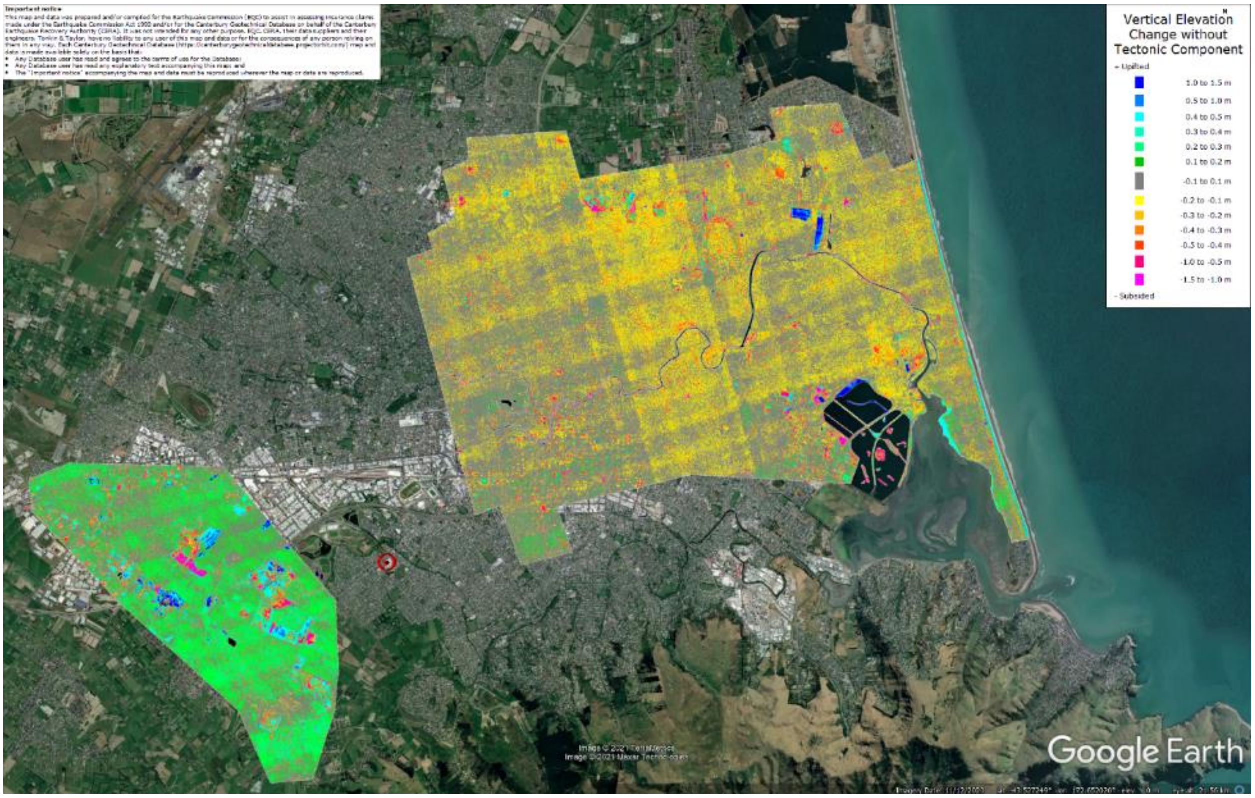

Figure 26: Vertical Ground Movements (Surface – Tectonic) for Sep 2010 Earthquake are not available.

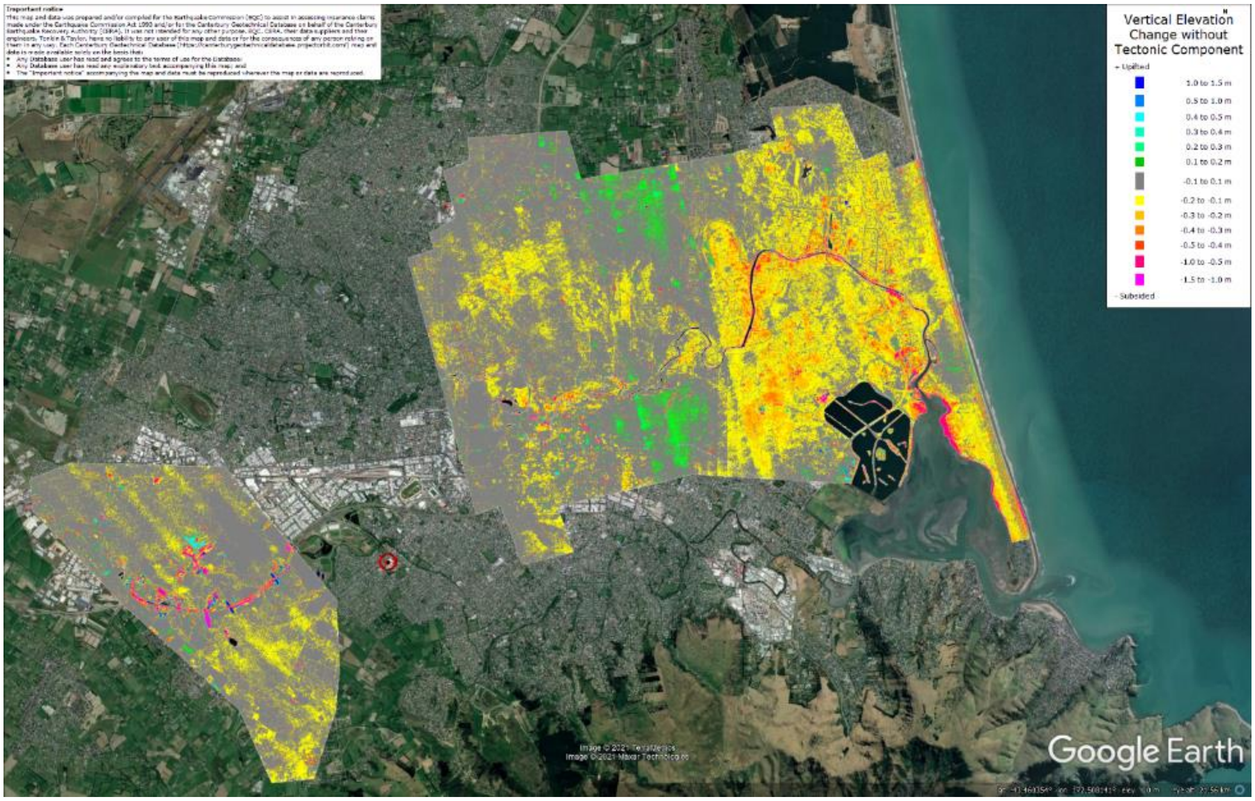

Figure 27: Vertical Ground Movements (Surface – Tectonic) for Feb 2011 Earthquake are not available.

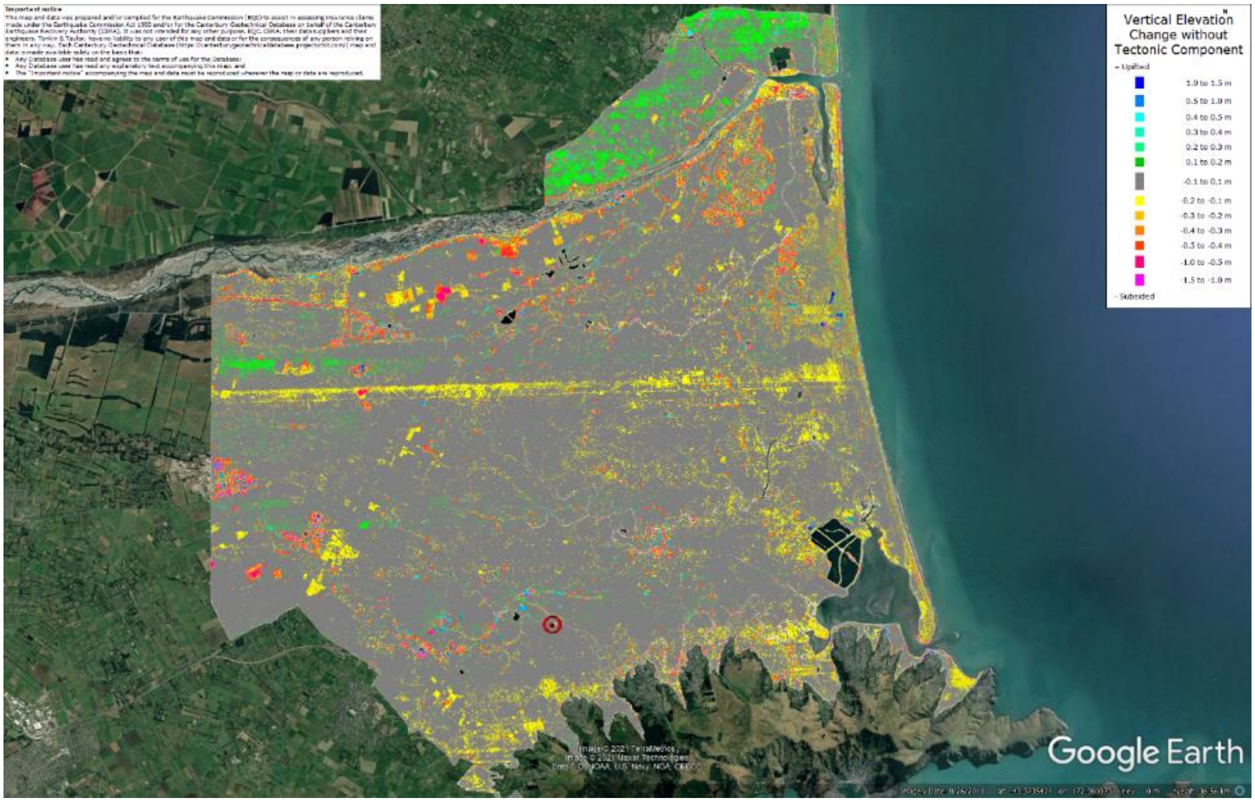

Figure 28: Vertical Ground Movements (Surface – Tectonic) for June 2011 Earthquake – the site is not in the apparent zone of overestimated or underestimated ground surface subsidence.

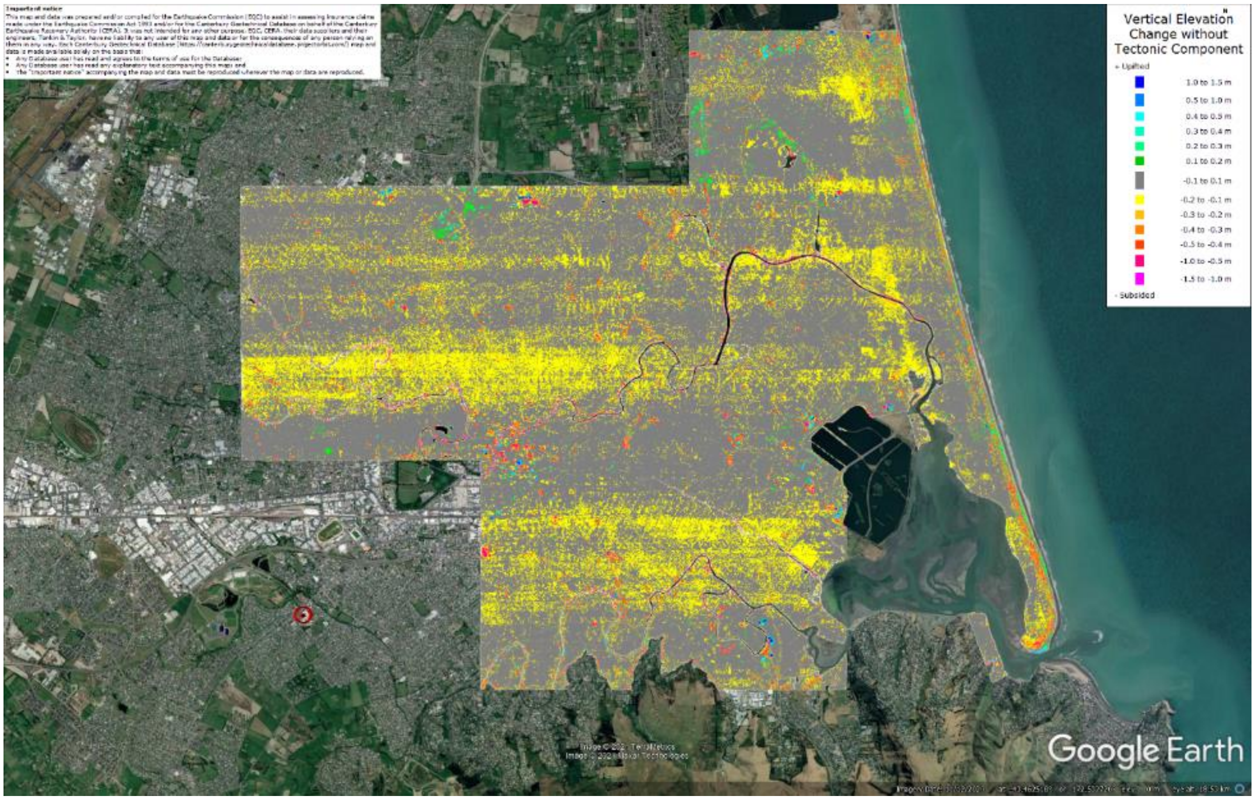

Figure 29: Vertical Ground Movements (Surface – Tectonic) for Dec 2011 Earthquake are not available.

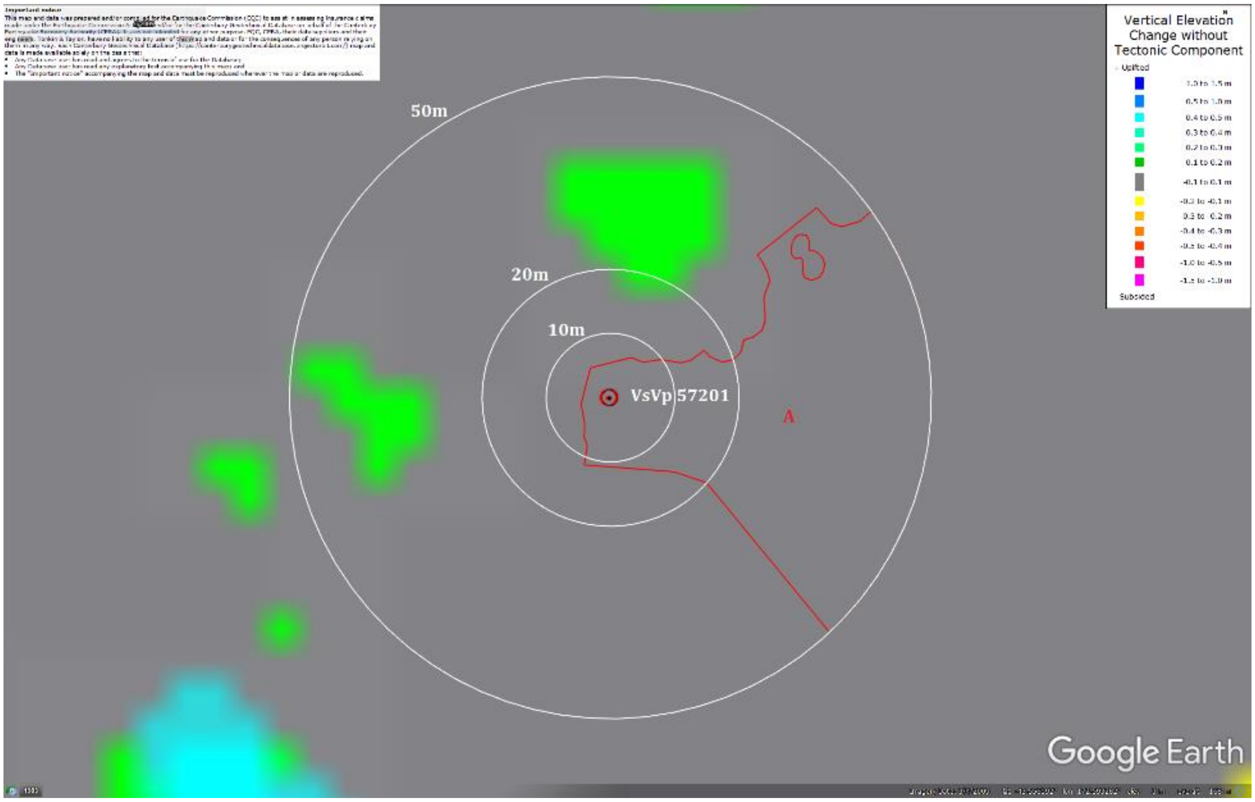

Figure 30: Ground surface subsidence without tectonic component for June 2011 Earthquake according to the LiDAR DEM.

Figure 31: No lateral spreading for Canterbury Earthquake Sequence.

Figure 32: Vertical tectonic movements for Sep 2010 Earthquake.

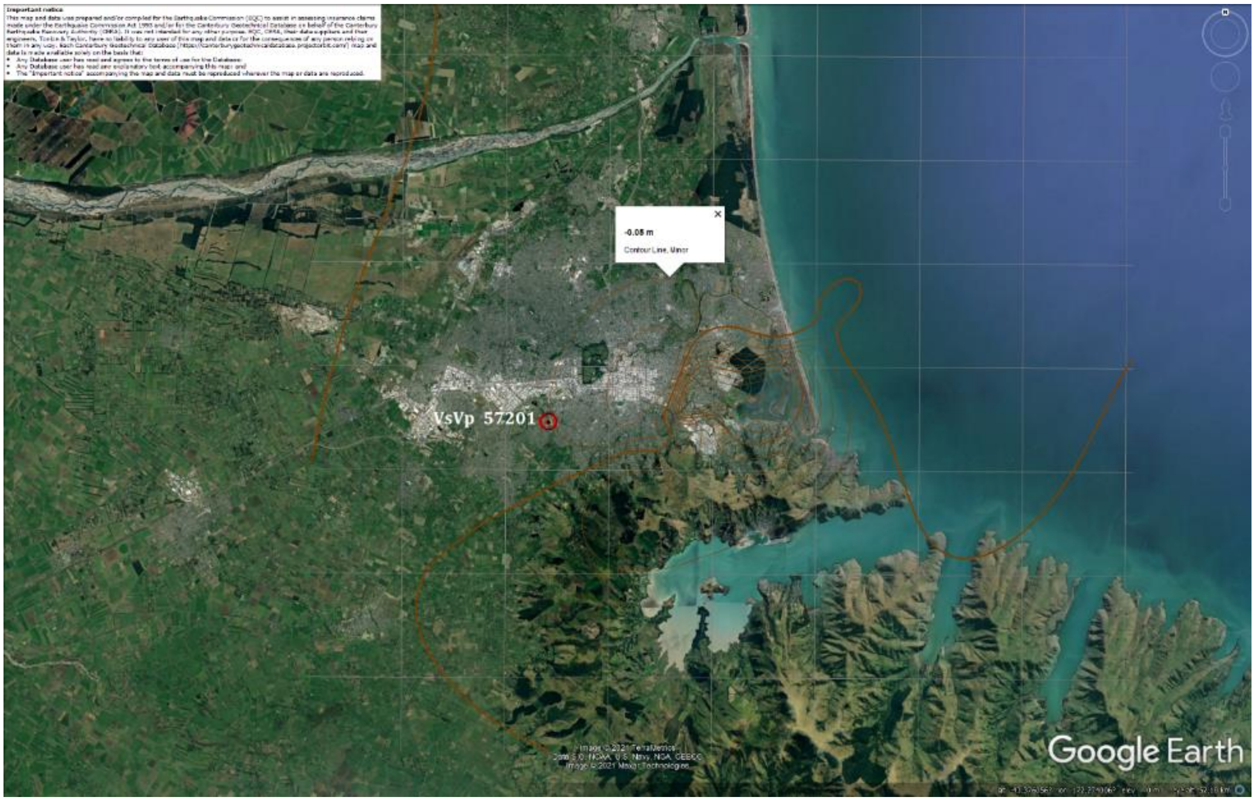

Figure 33: Vertical tectonic movements for Feb 2011 Earthquake.

Figure 34: Vertical tectonic movements for June 2011 Earthquake.

Figure 35: Vertical tectonic movements for Dec 2011 Earthquake.

Figure 36: Vertical tectonic movements for Canterbury Earthquake Sequence.

Figure 37: Aerial photograph showing the ejecta outline at the site for Feb-11 EQ.

Figure 38: Ground photograph showing ejecta at a nearby property (49 and 49A Halswell Rd).

Figure 39: PGA for Sep-10 EQ (st. dev. = 0.350-0.375 ln units).

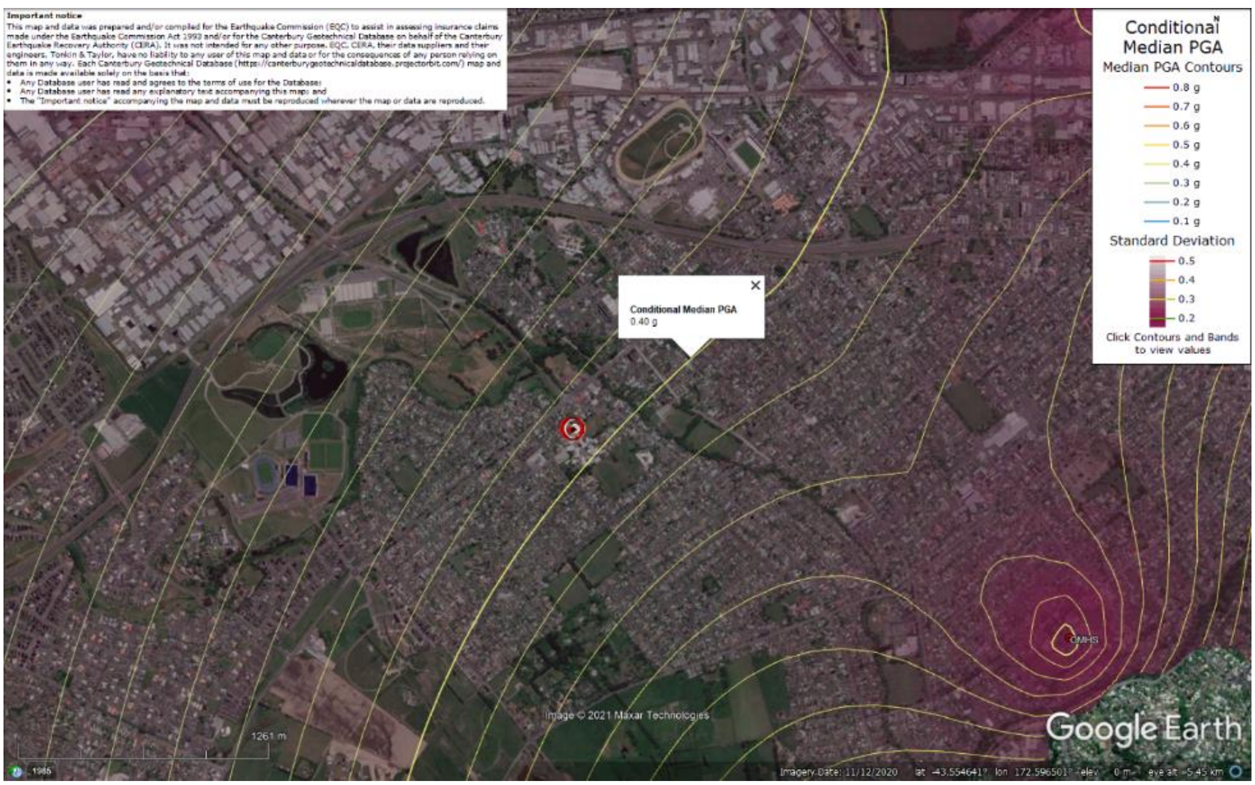

Figure 40: PGA for Feb-11 EQ (st. dev. = 0.375-0.400 ln units).

Figure 41: PGA for Jun-11 EQ (st. dev. = 0.400-0.425 ln units).

Figure 42: PGA for Dec-11 EQ (st. dev. = 0.250-0.275 ln units).

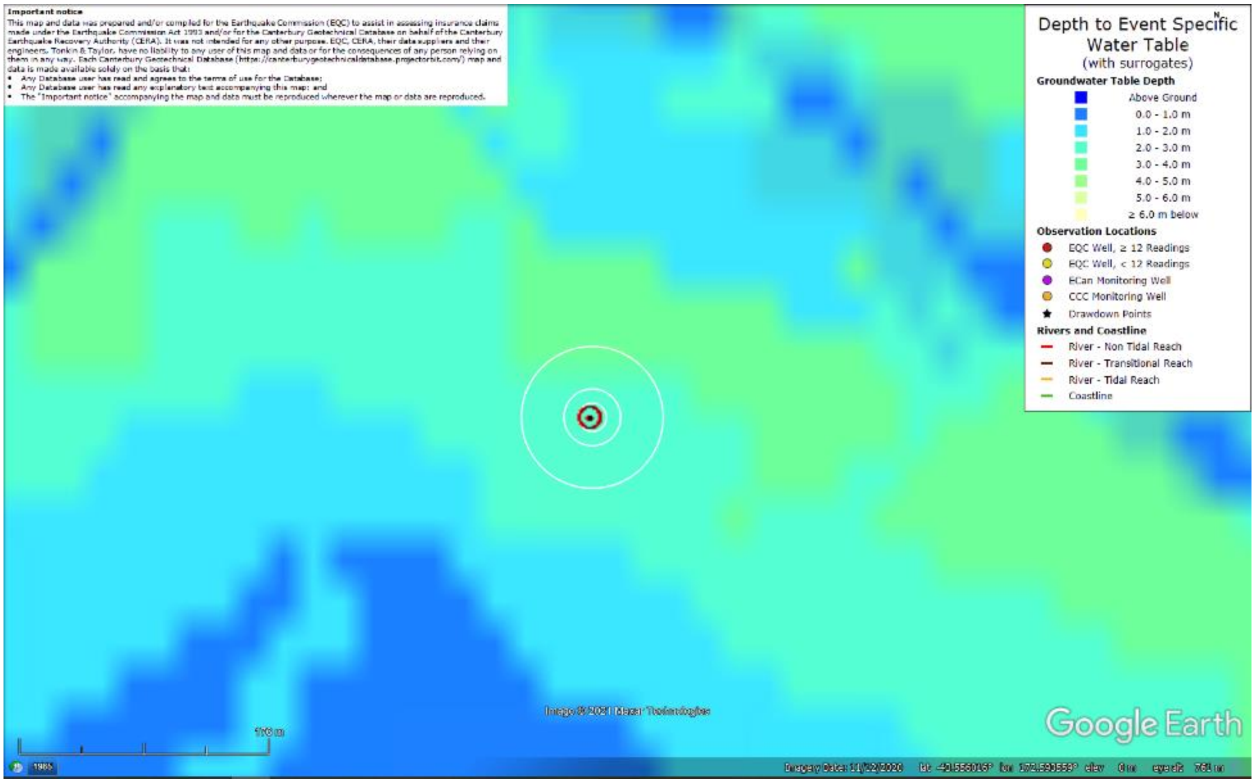

Figure 43: Depth to groundwater table for Sep-10 EQ.

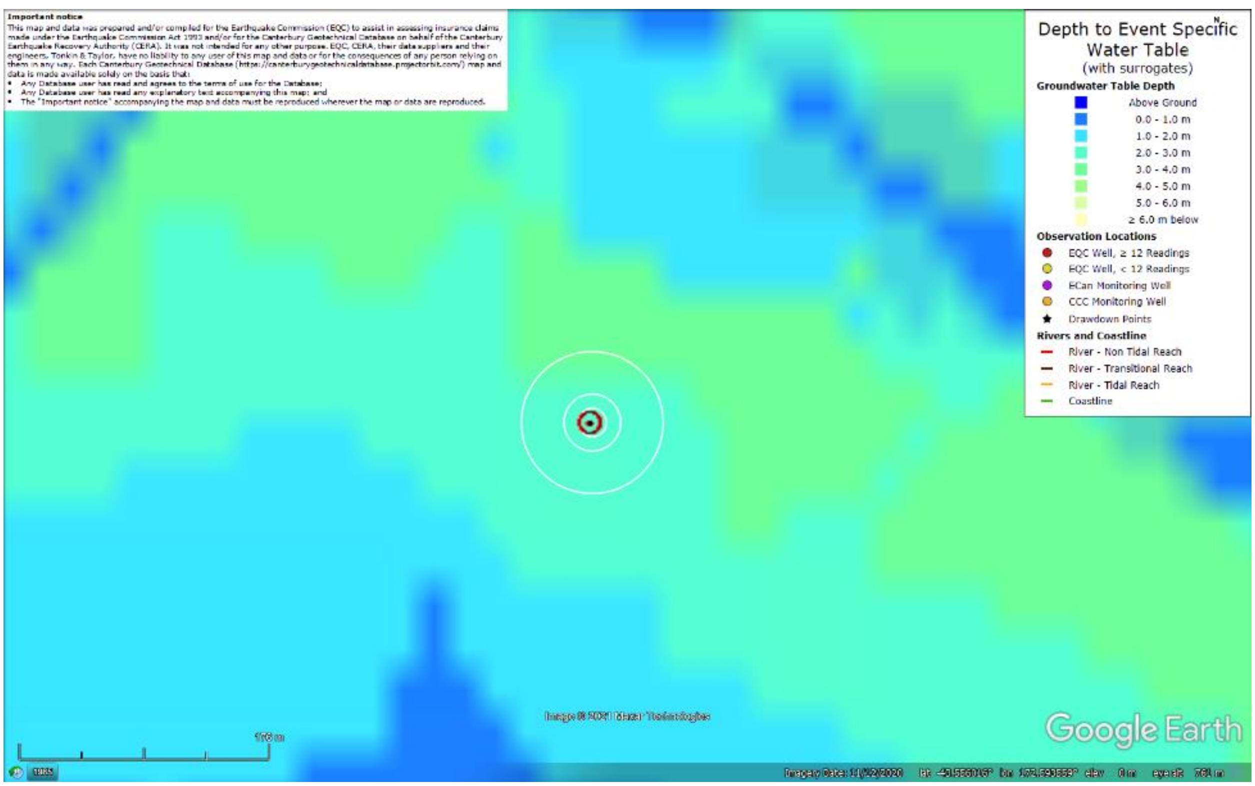

Figure 44: Depth to groundwater table for Feb-11 EQ.

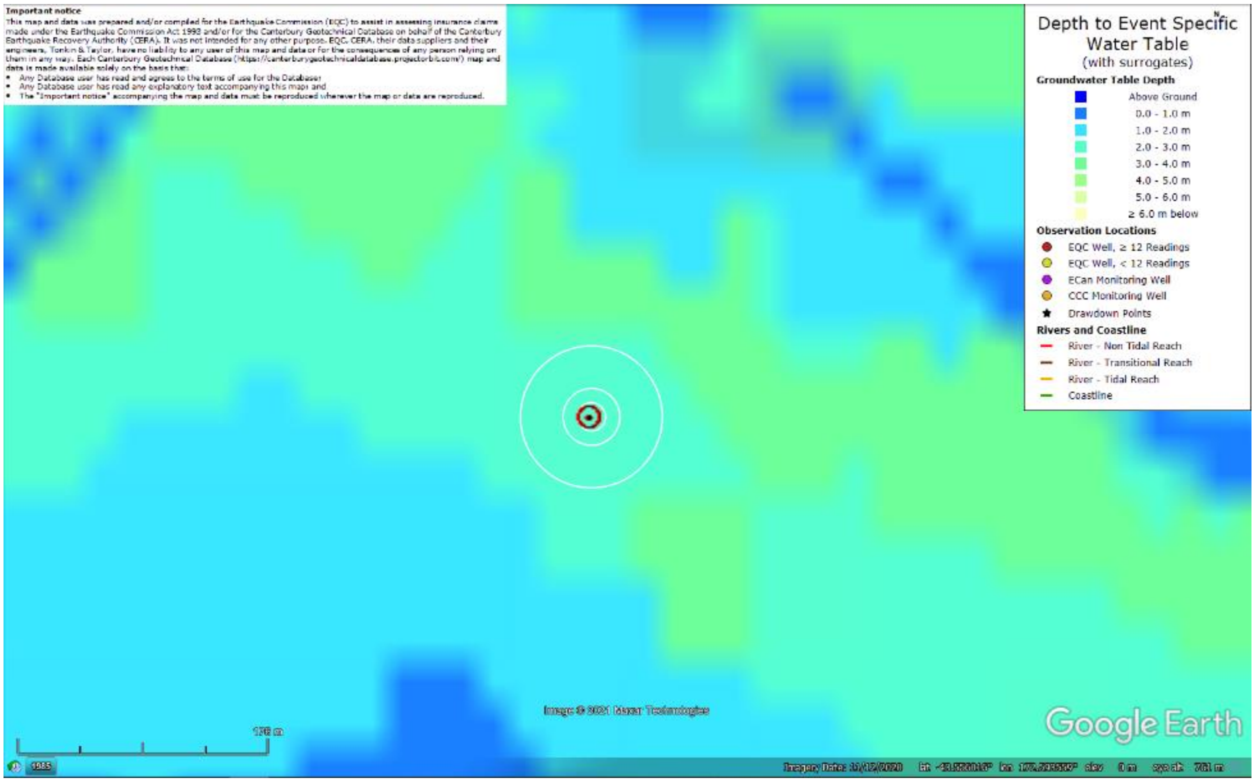

Figure 45: Depth to groundwater table for Jun-11 EQ.

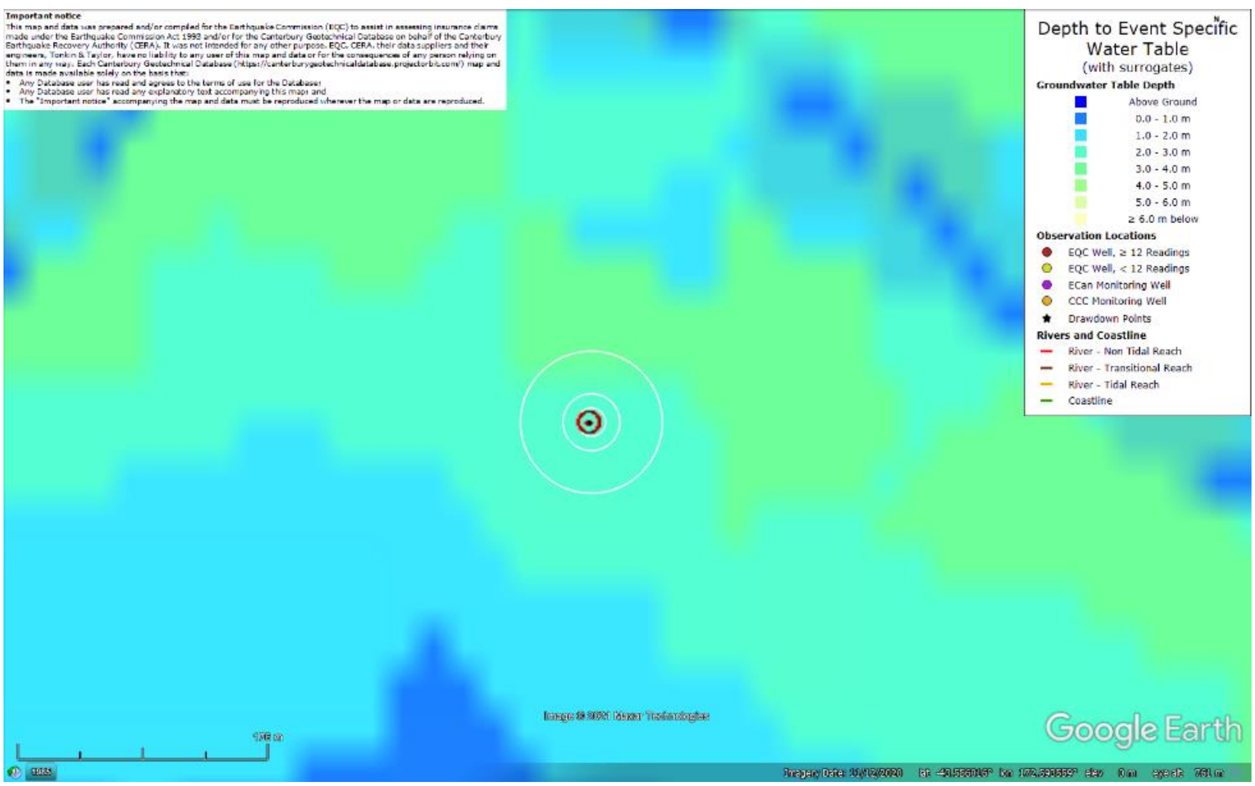

Figure 46: Depth to groundwater table for Dec-11 EQ.

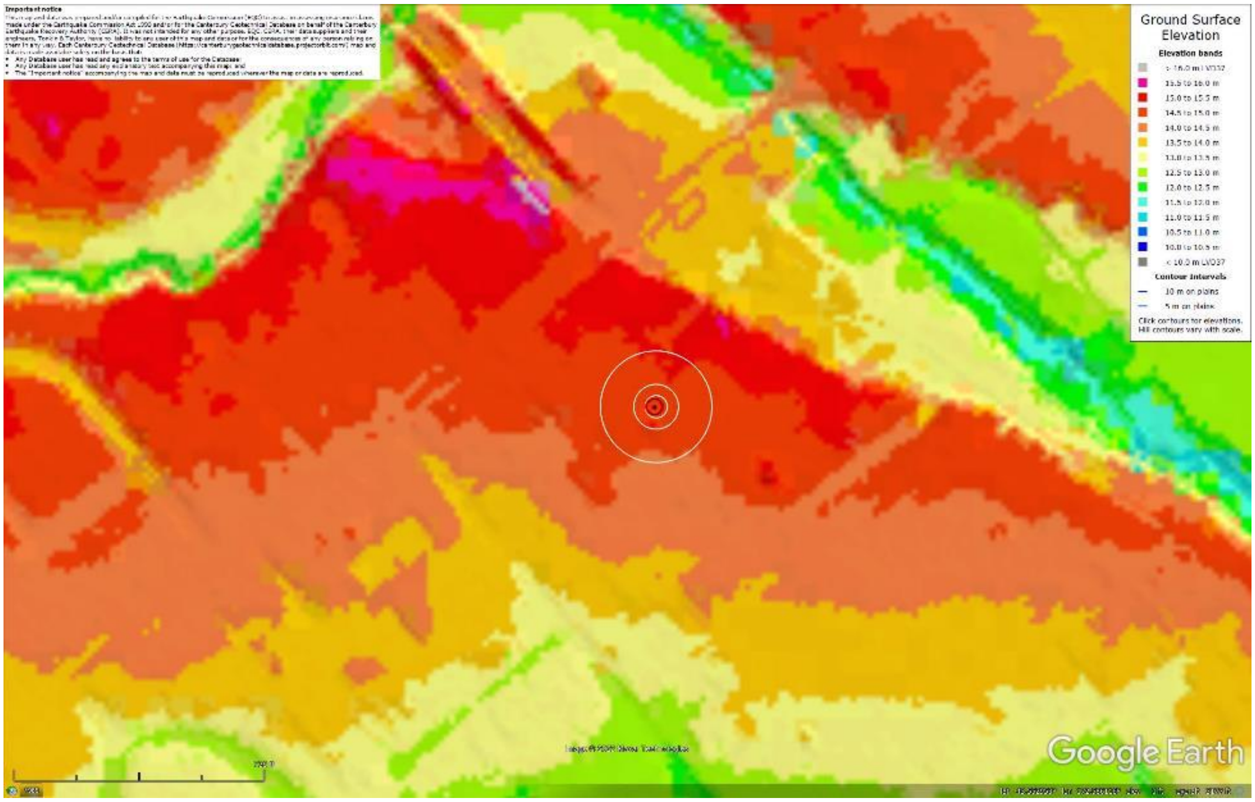

Figure 47: Ground surface elevation according to the Sep-11 LiDAR survey.

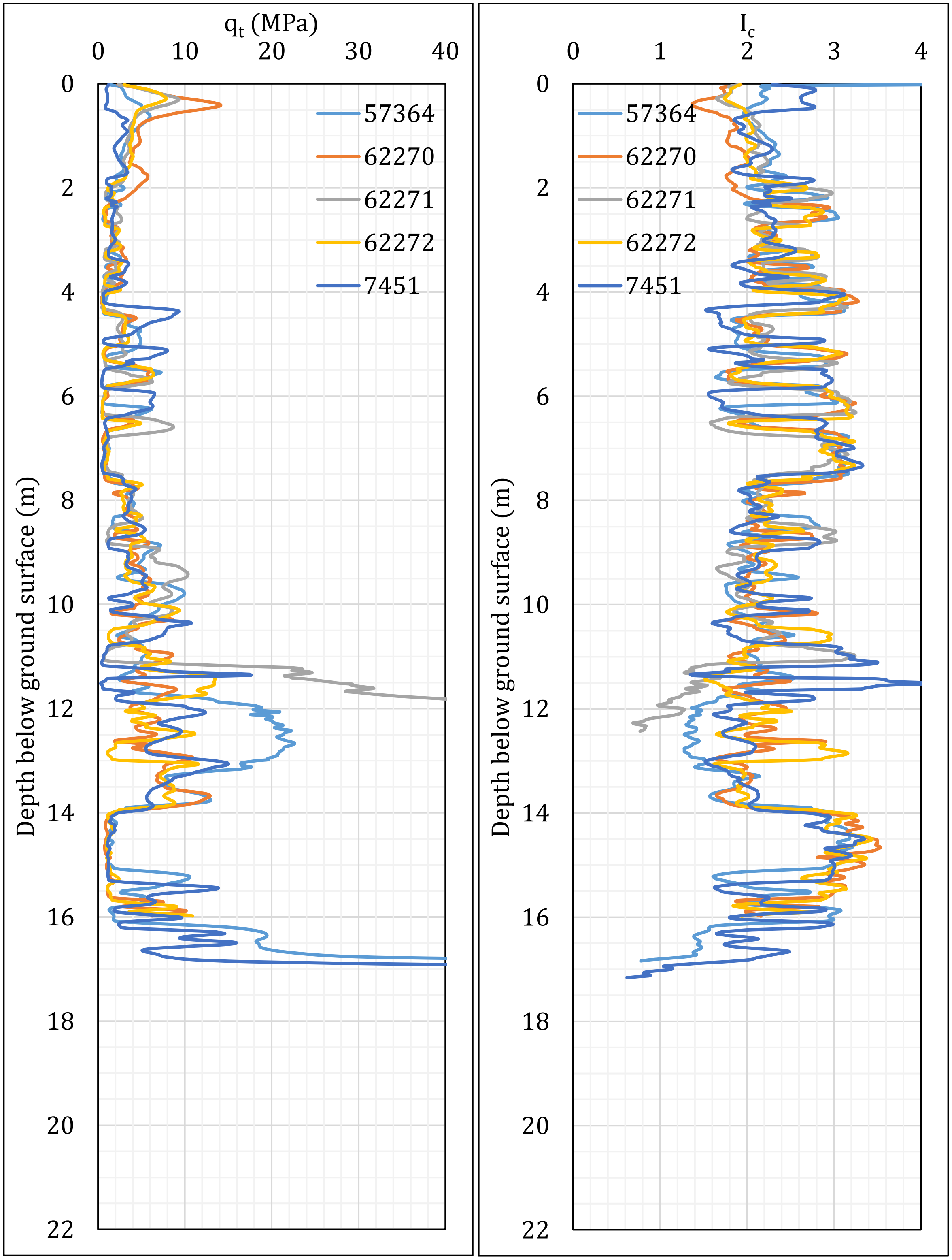

Figure 48: q_t and I_c profiles.

Note 6: The selection of CPTs for the area considered for settlement assessment (Figure 1) is based on the proximity of the CPTs to the considered areas. In accordance with that, the following table shows CPTs that were used for the volumetric settlement analysis in *Cliq v.3.0.3.2*, a CPT soil liquefaction software developed by GeoLogismiki. (The average volumetric settlements were reported in Table 8.)

Table 12: CPT profiles used in volumetric settlement analysis for Patch A selected for settlement assessment.

CPT ID No.	10-m buffer	20-m buffer	50-m buffer
57364 (56889)	✓	✓	✓
62270 (60921)		✓	✓
62271 (60922)			✓
62272 (60923)			✓
7451			

Notes: CPT 7451 was used to compute the volumetric settlement for CPTs 62270, 62271, and 62272 for the respective depth ranges: 16-20 m, 12.4-20 m, and 16-20 m; CPT 7451 is ~60 m to the NW from the center of the site.

Table 13: CPT-based results.

EQ Event	Parameter	CPT ID						
		57364	62270	62271	62272	7451*	$\Delta_{CPT62270/62272}$	$\Delta_{CPT62271}$
Sep-10	S_{V1D} (mm)	161	172	105	148	171	6	39
	LSN	22	23	18	20	23	0	3
	LPI	8	9	6	8	9	0	1
	LPI_{ish}	2	2	1	2	0	--	--
	$D_{FS<1}$ (m)	2.72	2.86	3.40	3.36	3.04	--	--
Feb-11	S_{V1D} (mm)	192	210	130	186	213	10	51
	LSN	28	30	22	27	31	1	4
	LPI	19	21	15	19	21	0	3
	LPI_{ish}	12	11	9	10	12	--	--
	$D_{FS<1}$ (m)	2.72	2.72	2.74	2.74	2.72	--	--
Jun-11	S_{V1D} (mm)	42	40	26	36	47	1	8
	LSN	5	5	4	5	6	0	0
	LPI	0	0	0	0	0	0	0
	LPI_{ish}	0	0	0	0	0	--	--
	$D_{FS<1}$ (m)	undet.	undet.	undet.	undet.	undet.	--	--
Dec-11	S_{V1D} (mm)	4	3	2	3	5	0	1
	LSN	0	0	0	0	1	0	0
	LPI	0	0	0	0	0	0	0
	LPI_{ish}	0	0	0	0	0	--	--
	$D_{FS<1}$ (m)	undet.	undet.	undet.	undet.	undet.	--	--

Notes: $D_{FS<1}$ = Depth to the first liquefiable layer (FS_L<1) that is at least 200-mm thick, as determined by the Boulanger and Idriss (2016) liquefaction-triggering procedure (P_L=50%, C_{FC}=0.13, and $I_{c,cutoff}$ =2.6), and exported from *Cliq v.3.0.3.2*; undet. = the specified soil layer was not detected; $\Delta_{CPT62270/62272}$ and $\Delta_{CPT62271}$ indicate the amount of S_{V1D}, LSN, and LPI added to CPTs 62270/62272 and 62271, respectively, due to the shallow penetration depths; * indicates that CPT 7451 is ~60 m to the NW from the center of the site.

Note 7: Based on the borehole log (BH 57257, Figure 1), the groundwater table is at a depth of 1.9 m below the ground surface. The soil profile consists of (1) organic silty, OL, topsoil to a depth of 0.25 m, (2) organic silt, OL, to a depth of 0.6 m, (3) silty fine sand, SM, to a depth of 2.05 m, (4) silt, ML, to a depth of 3.6 m, (5) silty fine sand, SM, to a depth of 3.85 m, (6) silt, ML, to a depth of 5.55 m, (7) silty fine sand, SM, to a depth of 5.85 m, (8) silt, ML, to a depth of 8.7 m, (9) silty fine sand, SM, to a depth of 9.95 m, (10) silty fine sand, SM, to a depth of 10.35 m, (11) silty fine sand, SP, to a depth of 11.2 m, (12) silt, ML, to a depth of 11.85 m, (13) fine sand, SP, to a depth of 12.1 m, (14) sandy fine to coarse gravel, GW, to a depth of 12.65 m, (15) fine to medium sand, SP, to a depth of 13.5 m, and (16) silt, ML, to a depth of 15.65 m (the end of the borehole). All soil layers, except the topsoil, are the Yaldhurst members of the Springston formation. According to BH 18081, which is ~60 m to the NW from the center of the site, the ML layer continues to a depth of ~16 m and overlies (17) silty fine to medium sand, SM, the Yaldhurst member of the Springston formation, to a depth of ~17 m, (18) silty fine to medium sand with minor gravel, SW, the Yaldhurst member of the Springston formation, to a depth of 17.2 m, and (19) Riccarton gravel, GW, to a depth of 20 m (the end of the borehole).

Note 8: The ejecta-induced free-field settlement provided in Table 11 is an areal average settlement due to ejecta, which is based on the total settlement assessment area, A_T (provided in Table 9 and repeated in Table 14). However, the considered area was not always covered completely with ejecta; thus, it is important to provide the localized ejecta-induced settlement, too. The localized settlement due to ejecta is estimated using photographic evidence only as

$$S_{E,P\_localized} = \frac{V_E}{A_E}$$

where V_E is the total volume of ejecta within A_T and A_E is the total coverage area of ejecta within A_T. Please note that the areal ejecta-induced settlement provided in Table 14 as S_{E,P_areal} is the same as $S_{E,P}$ in Table 11, which was estimated as

$$S_{E,P\_areal} = S_{E,P} = \frac{V_E}{A_T}$$

where V_E is the total volume of ejecta within A_T and A_T is the total settlement assessment area.

Table 14a: Areal and localized ejecta-induced settlement estimates for Patch A (10-m buffer) based on photographic evidence.

Earthquake Event	A_T (m²)	A_E (m²)	V_E (m³)	S_{E,P_areal} (mm)	$S_{E,P\_localized}$ (mm)
Sep-10	191	0	0	0	0
Feb-11	191	17.6	1.4-2.4	10±5	110±30
Jun-11	191	0	0	0	0
Dec-11	191	0	0	0	0

Notes: S_{E,P_areal} = $S_{E,P}$ reported in Table 11 = areal ejecta-induced settlement; $S_{E,P\_localized}$ = localized ejecta-induced settlement; A_T = total settlement assessment area; V_E = total volume of ejecta within A_T; A_E = total area of ejecta within A_T; The estimates of both areal and localized ejecta-induced settlement are rounded to the nearest 5; Final plus/minus values are also rounded to the nearest 5.

Table 14b: Areal and localized ejecta-induced settlement estimates for Patch A (20-m buffer) based on photographic evidence.

Earthquake Event	A_T (m^2)	A_E (m^2)	V_E (m^3)	S_{E,P_areal} (mm)	$S_{E,P\_localized}$ (mm)
Sep-10	398	0	0	0	0
Feb-11	379	60.9	3.5-5.8	10±5	75±20
Jun-11	398	0	0	0	0
Dec-11	398	0	0	0	0

Notes: S_{E,P_areal} = $S_{E,P}$ reported in Table 11 = areal ejecta-induced settlement; $S_{E,P\_localized}$ = localized ejecta-induced settlement; A_T = total settlement assessment area; V_E = total volume of ejecta within A_T; A_E = total area of ejecta within A_T; The estimates of both areal and localized ejecta-induced settlement are rounded to the nearest 5; Final plus/minus values are also rounded to the nearest 5.

Table 14c: Areal and localized ejecta-induced settlement estimates for Patch A (50-m buffer) based on photographic evidence.

Earthquake Event	A_T (m^2)	A_E (m^2)	V_E (m^3)	S_{E,P_areal} (mm)	$S_{E,P\_localized}$ (mm)
Sep-10	1893	0	0	0	0
Feb-11	1875	241	10.4-18.4	10±5	60±15
Jun-11	1893	0	0	0	0
Dec-11	1893	0	0	0	0

Notes: S_{E,P_areal} = $S_{E,P}$ reported in Table 11 = areal ejecta-induced settlement; $S_{E,P\_localized}$ = localized ejecta-induced settlement; A_T = total settlement assessment area; V_E = total volume of ejecta within A_T; A_E = total area of ejecta within A_T; The estimates of both areal and localized ejecta-induced settlement are rounded to the nearest 5; Final plus/minus values are also rounded to the nearest 5.

Summary 2:

The best estimate of the localized ejecta-induced free-field ground settlement at the Hillmorton High School site for the SEP 2010, FEB 2011, JUN 2011, and DEC 2011 earthquake is 0 mm, 110±30 mm, 0 mm, and 0 mm, respectively.